The EMBO Journal Vol. 21 No. 4 pp. 653–664, 2002

The centrosomal protein TACC3 is essential for hematopoietic stem cell function and genetically interfaces with p53-regulated apoptosis

Roland P.Piekorz[1,2], Angelika Hoffmeyer[1,2], Christopher D.Duntsch[2,3], Catriona McKay[1,2], Hideaki Nakajima[2,4], Veronika Sexl[2,5], Linda Snyder[1,2], Jerold Rehg[6] and James N.Ihle[1,2,3,7]

[1]Howard Hughes Medical Institute, [2]Department of Biochemistry, [6]Department of Pathology, St Jude Children's Research Hospital, Memphis, TN 38105 and [3]Department of Biochemistry, University of Tennessee Health Science Center, Memphis, TN 38063, USA

[4]Present address: Blood Center, Keio University School of Medicine, 35 Shinanomachi, Shinjuku-ku, Tokyo 160, Japan
[5]Present address: Department of Pharmacology, University of Vienna, A-1090 Vienna, Austria

[7]Corresponding author
e-mail: james.ihle@stjude.org

A.Hoffmeyer, C.D.Duntsch, C.McKay and H.Nakajima contributed equally to this work

TACC3 is a centrosomal/mitotic spindle-associated protein that is highly expressed in a cell cycle-dependent manner in hematopoietic lineage cells. During embryonic development, TACC3 is expressed in a variety of tissues in addition to the hematopoietic lineages. *TACC3* deficiency causes an embryonic lethality at mid- to late gestation involving several lineages of cells. Hematopoietic stem cells, while capable of terminal differentiation, are unable to be expanded *in vitro* or *in vivo* in reconstitution approaches. Although gross alterations in centrosome numbers and chromosomal segregation are not observed, *TACC3* deficiency is associated with a high rate of apoptosis and expression of the p53 target gene, $p21^{Waf1/Cip1}$. Hematopoietic stem cell functions, as well as deficiencies in other cell lineages, can be rescued by combining the *TACC3* deficiency with *p53* deficiency. The results support the concept that TACC3 is a critical component of the centrosome/mitotic spindle apparatus and its absence triggers p53-mediated apoptosis.

Keywords: apoptosis/centrosome/hematopoiesis/p53/TACC3

Introduction

The centrosome is essential for the organization of the bipolar mitotic spindle during cell division. The functions of centrosome/spindle apparatus-associated proteins can be envisioned to be structural, e.g. γ-tubulin, forming ring complexes that are associated with centrosomes (Moritz and Agard, 2001) and mediate the assembly and maintenance of the spindle apparatus; functional, e.g. motor proteins like dynein or CENP-E (Compton, 2000) providing the reactions necessary for chromosomal positioning, attachment and segregation; or regulatory, e.g. the signaling proteins Mad2 and Bub1 as components of the spindle assembly checkpoint, which senses unattached chromosomes and therefore the integrity of the mitotic process (Shah and Cleveland, 2000). During the mitotic phase, a large number of regulatory proteins become associated with the centrosome/spindle apparatus including the tumor suppressor gene products Rb (Thomas *et al*., 1996), BRCA1 (Hsu and White, 1998) and p53 (Morris *et al*., 2000). Also associated with the centrosome/spindle apparatus during mitosis are members of a recently identified and evolutionarily conserved protein family, referred to as the TACC (transforming acidic coiled-coil-containing) family. These proteins are characterized by a unique C-terminal coiled-coil domain of ~200 amino acids, but lack significant homology outside of this domain (Gergely *et al*., 2000a).

The mammalian TACC family consists of three genes. *TACC1*, the first family member identified, was discovered as a gene amplified in breast cancer (Still *et al*., 1999a). A related gene (*AZU-1*/*TACC2*) was identified by homology and its expression was found to be reduced in breast cancer (Chen *et al*., 2000). ECTACC, a splice variant of the human *TACC2* gene, shows increased expression in endothelial cells upon erythropoietin (Epo) treatment and is predominantly found in heart and skeletal muscle (Pu *et al*., 2001). Lastly, the *TACC3* gene was identified in a yeast two-hybrid screen for genes encoding ARNT-interacting proteins (Sadek *et al*., 2000), by gene homology to *TACC1* (Still *et al*., 1999b), as an Epo-induced gene in erythroid progenitors (McKeveney *et al*., 2001) or, in our case, as a Stat5-interacting gene product in yeast two-hybrid screens (our unpublished data).

In addition to the mammalian genes, a *Drosophila* TACC (*dTACC*) was identified as a centrosomal protein that interacts with microtubules and plays an essential role in normal spindle function during embryogenesis (Gergely *et al*., 2000a). A 10-fold reduction in *dTACC* expression leads to mitotic defects and death during early embryogenesis and female sterility in adults. Localization of the protein to the mitotic spindle requires the C-terminal coiled-coil domain and this domain is sufficient to target heterologous proteins to the centrosomal complex (Gergely *et al*., 2000a). Recent studies have indicated that the localization may be mediated by interaction with another centrosomal/spindle apparatus-associated and evolutionarily conserved protein, Msps/XMAP215/ch-TOG (Cullen and Ohkura, 2001; Lee *et al*., 2001). Since Msps/XMAP215/ch-TOG associates with microtubuli and localizes preferentially at the centrosome, these studies provided a mechanism linking the dTACC–Msps complex to the stability of centrosomal microtubuli in *Drosophila* embryos. Lastly, in *Xenopus*, the TACC-related gene is

termed *Maskin* based on its isolation in a complex containing CPEB (cytoplasmic polyadenylation element binding factor) and eIF-4E-associated protein during oocyte maturation (Stebbins-Boaz *et al*., 1999). A role for Maskin in translational regulation has been proposed since this complex localizes certain mRNAs, such as cyclin B1, to the mitotic apparatus/centrosome and thereby allows the regulation of mRNA translation with cell cycle progression by the integrity of the mitotic machinery (Groisman *et al*., 2000).

The functions of the mammalian TACC proteins are largely unknown. The identification of *TACC1* as a highly amplified gene in breast cancer tissues suggests a role in malignant transformation (Still *et al*., 1999a). In contrast, a *TACC2* splice variant is expressed at low levels in tumorigenic cell lines and its overexpression reduces the malignant phenotype leading to the suggestion that *TACC2* might function as a tumor suppressor gene (Chen *et al*., 2000). Finally, *TACC3* has been proposed to play a role in hypoxic responses based on its association with *ARNT*, a gene essential for hypoxic responses (Sadek *et al*., 2000). Irrespective, the characteristic localization of all mammalian members at the centrosome/mitotic spindle indicates a role of these proteins in chromosomal segregation and cell division (Gergely *et al*., 2000b).

To explore the function of the mammalian *TACC3* gene, we have characterized the lineage specificity of its expression, explored the cell cycle dependence for its expression in lymphocytes and examined its subcellular localization. To further establish the physiological relevance of the gene we have developed mutant strains of mice lacking the gene. Together our studies demonstrate that *TACC3* is highly tissue specific in its normal pattern of expression and within the lymphoid lineages it is specifically expressed during the $S/G_2/M$ phases of the cell cycle at which time it is associated predominantly with the mitotic spindle and centrosomal regions. The absence of *TACC3* results in an embryonic lethality, demonstrating the essential role of TACC3 protein for cell expansion during embryonic development and in hematopoiesis. The defects caused by *TACC3* deficiency are obviated on a *p53*-deficient background, supporting the concept that the TACC3 protein is a critical sensor of the mitotic apparatus that couples to a p53-dependent pathway to regulate cell cycle progression.

Results

Lineage and cell cycle-dependent expression of TACC3

As illustrated in Figure 1A, relatively few adult tissues express *TACC3* mRNA with the exception of lung and high levels of expression in testis. However, *TACC3* is expressed at high levels in all hematopoietic sites including bone marrow, fetal liver, thymus and spleen. This pattern of expression is quite distinct from that of *TACC2* (Figure 1A) or *TACC1* (not shown), which are not expressed in hematopoietic tissues. In particular, *TACC2* is more widely expressed, with the highest levels of transcripts being present in heart and muscle. Two mRNAs of 4 and 10 kb are seen in most tissues although the ratios vary. Muscle and heart predominantly express the 10 kb transcript while the 4 kb transcript is more ubiquitously expressed. These results are similar to the pattern of expression of the *TACC2* mRNA in human tissues (Pu *et al*., 2001).

In T lymphocytes, *TACC3* expression is cell cycle regulated (Figure 1B). In these experiments, T cells were expanded *in vitro* with anti-CD3 and interleukin-2 (IL-2) starved of cytokines overnight and restimulated with IL-2. As illustrated, starved T cells (st) have little *TACC3* gene transcripts but expression is induced following stimulation with IL-2. The highest levels of expression occurred at 18 h following stimulation at which time 60% of the cells were through the S-phase. Comparable results were obtained with naïve T cells or B cells stimulated with anti-CD3 and IL-2 or anti-IgM and IL-4, respectively (data not shown). Therefore, *TACC3* is a cell cycle-regulated, non-immediate early gene in the response of lymphocytes to cytokines.

During embryonic development, *TACC3* gene transcripts are detected starting at E7, strongly upregulated at E11, and expression is maintained throughout the remainder of embryogenesis (Figure 1A). At E18.5, expression was detected by *in situ* hybridization in a variety of developing organs/tissues including the neuroepithelium of the forebrain, epithelial cells of the gut as well as epithelial cells of other organs (data not shown). The highest levels of *TACC3* expression were found in the fetal liver throughout the last half of embryogenesis and in the developing fetal thymus (data not shown). In contrast, only low levels of the two *TACC2* transcripts are observed during embryonic development. The results support the conclusion that *TACC3* is highly expressed within the hematopoietic lineages as well as in developing epithelial layers of various organs.

Localization of TACC3 to the centrosome/mitotic apparatus

To establish the subcellular localization of the murine TACC3 protein, exponentially growing mouse embryonic fibroblasts were stained with purified anti-mouse TACC3 antibodies. As illustrated in Figure 2, in mitotic cells, TACC3 protein was associated predominantly with the centrosomal region and mitotic spindle and colocalized with α-tubulin on spindle microtubules and γ-tubulin in the centrosomal region (data not shown). In interphase cells, TACC3 localizes to the cytoplasm and perinuclear region (data not shown). These results are comparable to recent studies examining the subcellular localization of the human TACC3 protein (Gergely *et al*., 2000b).

TACC3 deficiency causes growth retardation and embryonic lethality

The physiological functions of TACC3 were assessed by deriving *TACC3*-deficient mice. The targeting vector (Figure 3A) was designed to disrupt the third exon and would be predicted to alter splicing in such a manner as to generate a null mutation. Heterozygous *TACC3*-deficient mice were phenotypically normal and were bred to obtain homozygously null mice. As detailed below, homozygous *TACC3* deficiency was associated with embryonic lethality at mid- to late gestation. Analysis of RNA and protein from fetal livers, or total embryo extracts, of homozygous mutant mice is illustrated in Figure 3C and D. No transcripts were detected that hybridized with a *TACC3*

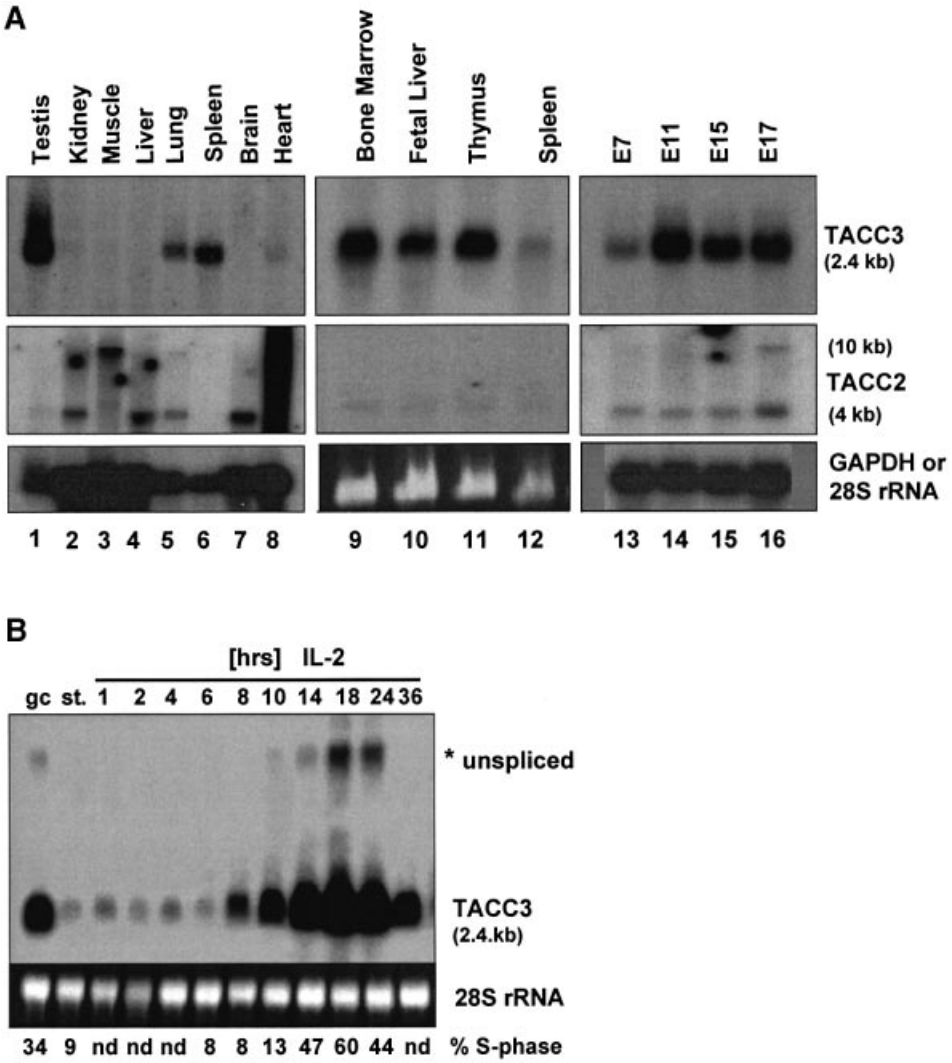

Fig. 1. Lineage-dependent expression of the *TACC3* gene. (**A**) The distribution of *TACC3* and *TACC2* transcripts in tissues from adult mice (lanes 1–12) and during embryogenesis (days 7–17 of development; lanes 13–16) was determined by northern blot analysis [lanes 1–8 and 13–16, poly(A)$^+$ mRNA; 9–12, total RNA]. (**B**) Preactivated T cells growing in IL-2 (gc) were starved overnight (st.) and restimulated with IL-2 for the indicated periods of time. *TACC3* mRNA levels were analyzed by northern blotting. The percentage of cells in S phase of the cell cycle is indicated (nd, not determined). Hybridization for *GAPDH* [lanes 1–8 and 13–16 in (A)] or staining of 28S rRNA with ethidium bromide [lanes 9–12 in A, lanes in (B)] was used to control RNA loading.

cDNA probe, indicating that the genomic modifications resulted in a null mutation. Consistent with the RNA data, immunoprecipitation and western blotting with an antiserum against an N-terminal peptide that would be retained in an alternatively spliced RNA capable of encoding an internally deleted TACC3 protein, failed to detect any immunoreactive protein. Together the results demonstrate that the mutated locus creates a TACC3 protein null mutant strain.

The distributions of genotypes of embryos from breedings of heterozygous mutant mice at various stages of embryonic development are tabulated in Table I. At mid-gestation (E9.5–11.5) the frequency of homozygously null embryos is close to the expected distribution. However, the frequency subsequently decreases to ~40% of that expected from normal Mendelian distribution. This frequency is maintained until late in embryogenesis when a second period of embryonic lethality occurs such that at birth the frequency of homozygous null mutants is only 5% of that expected and none have been born alive among >55 litters that were closely monitored. Morphologically, *TACC3*-deficient embryos were readily detected by a striking growth retardation (Figure 4) throughout the second half of embryogenesis. Approximately two-thirds of the homozygous null embryos displayed a severe facial cleft. Histological sections from homozygous null embryos revealed normal organ structure, although most organs were smaller and underdeveloped relative to the controls (data not shown).

Hematopoietic deficiencies of TACC3 null embryos

The high levels of expression of *TACC3* in fetal liver prompted us to examine *TACC3*-deficient hematopoietic cells in detail. As illustrated in Table II, there was a profound deficiency in hematopoietic stem cell colony forming activity although the total number of fetal liver cells was only one-half to one-quarter of that of controls. In general, the frequency of colony forming cells in

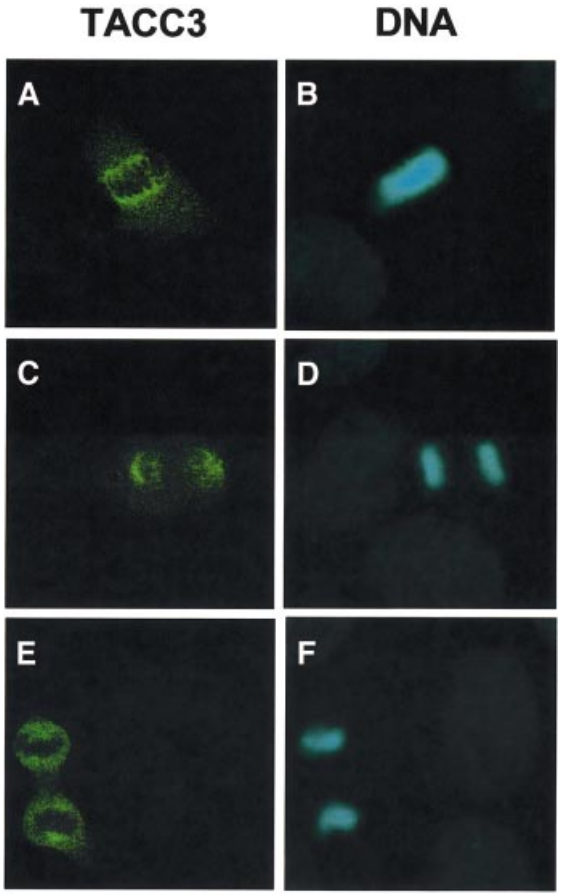

Fig. 2. Centrosomal localization of TACC3 during mitosis. Immunofluorescence detection of endogenous TACC3 protein (**A**, **C** and **E**) and DNA (**B**, **D** and **F**) in mouse embryo fibroblasts during different phases of mitosis (metaphase, A and B; anaphase, C and D; and telophase, E and F).

TACC3-deficient fetal livers was 1–5% of that of controls including cells responding to stem cell factor (SCF), IL-3 or mixtures of these cytokines with IL-6 and Epo. Among the various lineages, the least affected progenitors were those committed to the erythroid lineage (CFU-E) and responsive to Epo as a single cytokine. However, the more primitive progenitors of the erythroid lineage (BFU-E) were greatly reduced with *TACC3* deficiency. In addition to a numerical reduction, the sizes of the individual colonies, in all conditions, were significantly smaller than controls (data not shown). In the lymphoid lineage, *TACC3* deficiency resulted in a striking reduction in thymus size and in the number of fetal thymocytes, although the residual cells expressed both CD4 and CD8 (Figure 5A and B). Together the data indicate that hematopoietic stem cell differentiation is unaffected although the ability to proliferate and to expand is dramatically reduced.

To further assess hematopoietic stem cell function, reconstitution experiments were used. Fetal liver cells from *TACC3*-deficient embryos were unable to reconstitute the myeloid lineages in lethally irradiated wild-type mice at either 2.5×10^6 or 2.5×10^7 transferred fetal liver cells/recipient (data not shown). The latter cell dose is ~20-fold higher than that required for 80% reconstitution of lethally irradiated mice with wild-type cells. Fetal liver cells from *TACC3*-deficient embryos were also unable to reconstitute the lymphoid lineage in sublethally irradiated mice that had greatly reduced lymphoid lineage cells due to *Jak3* deficiency (data not shown). The results indicate that *TACC3* deficiency resulted in a cell intrinsic defect in hematopoietic stem cell function.

The possibilities existed that the decreased proliferative capacity of *TACC3*-deficient cells was associated with a decreased rate of proliferation and/or an increased rate of apoptosis. To begin to distinguish between these possibilities, the frequency of apoptotic cells was examined at various stages of development. As illustrated in Figure 6, a dramatic increase in TdT-mediated dUTP nick end labeling (TUNEL)-positive cells was evident in the forebrain, gut and fetal liver as well as in other tissues (data not shown). To determine whether the increased apoptosis might be associated with the activation of p53, the expression of $p21^{waf1/cip1}$ was examined in fetal liver cells. Consistent with a potential role for p53 in the increased apoptosis, high levels of $p21^{waf1/cip1}$ protein were present in extracts of fetal livers from *TACC3*-deficient embryos (E16–E18.5) but not in extracts from wild-type fetal livers (Figure 6G).

p53 deficiency rescues hematopoietic stem cell function of TACC3-deficient cells

The above results were consistent with the concept that the absence of *TACC3* was inducing a p53-mediated apoptosis. To explore this possibility, the *TACC3* deficiency was crossed onto a *p53* deficiency. In order to exclude background modifier genes on the p53 background, primarily progeny from a $TACC3^{+/-}$; $p53^{+/-}$ F_1 intercross were examined, including mice that were genotypically $TACC3^{+/+}$; $p53^{-/-}$. As illustrated in Figure 7A, *p53* deficiency had a significant effect on the embryonic lethality. For example, during late embryogenesis, the ratio of the actual to the expected number of viable embryos increased from 0.49 to 1.1 (E16–E17.5) and from 0.22 to 0.92 (E18–E19) when *TACC3*-deficient embryos were heterozygously deficient for *p53*. Equally striking, *TACC3*-deficient embryos that were homozygously deficient for *p53* were somewhat more susceptible to embryonic lethality than *p53* wild-type embryos (reduction to 0.17 for E16–E17.5). The results suggest that the interaction of p53 with TACC3 is complex, with a reduction of p53 being beneficial while the complete absence increases lethality. Perhaps the most striking result, however, was the ability to obtain viable mice at a low frequency that were genotypically either heterozygous or homozygous for *p53* deficiency and were homozygously *TACC3* deficient (Figure 7B and C). This contrasts with the lack of any viable mice from over 55 litters examined to date of *TACC3*-deficient and $p53^{+/+}$ embryos from the F_1 intercross.

Viable offspring from the above cross were further characterized. Characteristically, all the mice had a kinky tail (Figure 7B and C) and males and females were sterile. Peripheral blood patterns, analyzed by FACS with lineage specific markers, were found to be normal (data not shown). Moreover, the ability of T cells to proliferate in response to anti-CD3 and IL-2 was normal (data not shown). Lastly, bone marrow colony forming activity was

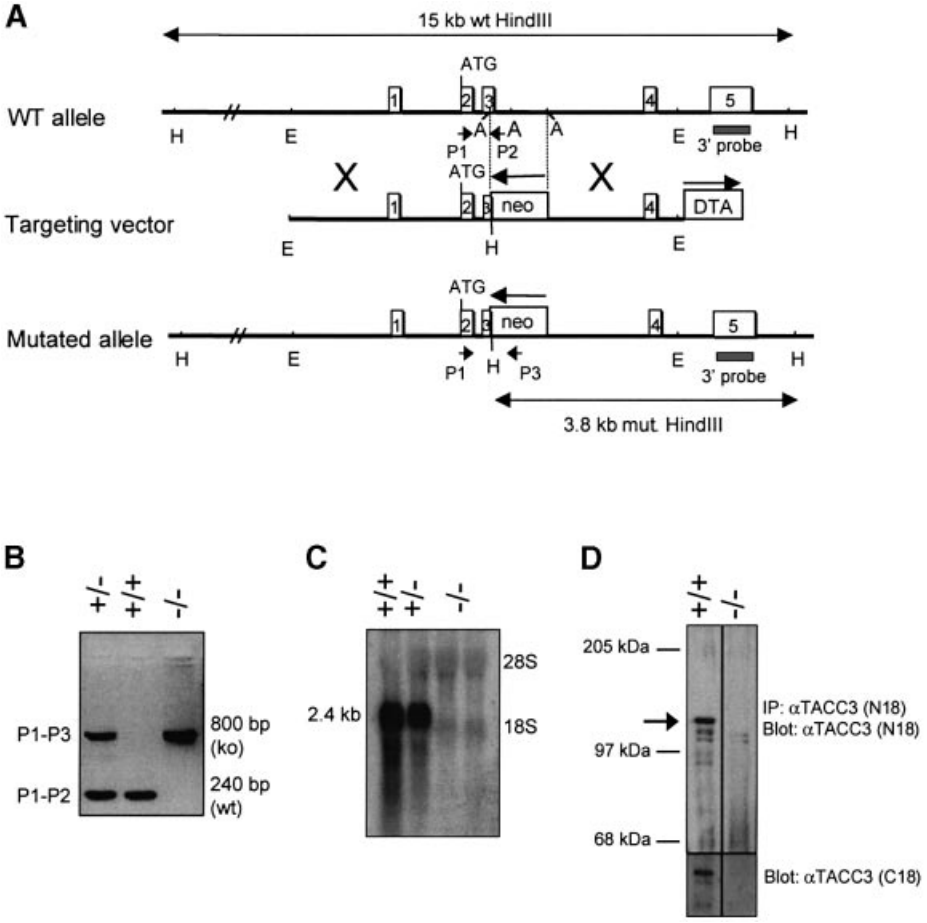

Fig. 3. Targeted disruption of the *TACC3* gene. (**A**) Structure and targeting strategy of the *TACC3* locus. Empty boxes indicate exons 1–5 of the *TACC3* locus. The locations of the 3′ external probe and PCR primers for genotyping are indicated. ATG denotes the first coding exon. Restriction enzyme sites are as follows: A, *Afl*II; E, *Eco*RI; H, *Hin*dIII. (**B**) Screening PCR of F_1 mice and TACC3-targeted embryos for the presence of the disrupted allele. (**C**) Analysis of *TACC3* mRNA and protein expression (**D**) in *TACC3*-deficient embryos. Total RNA was isolated from fetal liver cells, whereas protein lysates were obtained from whole embryos and analyzed by IP/western blotting.

Table I. Genotypic distribution of embryos and mice from TACC3 heterozygous intercrosses

Stage	No. of litters	Total No.	TACC3$^{(+/+)}$	TACC3$^{(+/-)}$	TACC3$^{(-/-)}$	(–/–) %
9.5–10.5	7	68	24	28	16	23.5
10.5–11.5	6	45	8	28	9	20
12–12.5	10	74	25	41	8	10.8
13–13.5	24	165	53	93	19	11.5
14–15.5	42	302	104	170	28	9.3
16–17.5	31	189	53	113	23	12.2
18–19	31	215	73	130	12	5.6
Newborns	55	297	88	209	(4)[a]	(1.3)

Embryos were collected between days 9.5 and 19.0 of pregnancy from TACC3$^{(+/-)}$ intercrosses. The frequency of mutant embryos is indicated in the table as a percentage of the total number of embryos analyzed.
[a]Newborns found on day 1 were dead.

normal. Among the three *TACC3* and *p53* double deficient mice that were allowed to age, one developed a sarcoma, one developed both a sarcoma and a thymoma while the third animal developed a peripheral T-cell lymphoma, all at ~5 months of age. The results indicate that *TACC3* deficiency does not increase or decrease the tumor-prone phenotype associated with *p53* deficiency.

The above results demonstrated that a reduction in p53 could significantly rescue the hematopoietic system and thus raised the possibility that the inefficient rescue of viable offspring might be due to other limiting cell types during embryogenesis. We therefore examined the ability of fetal liver stem cells to rescue the hematopoietic system and thereby allow the survival of lethally irradiated mice. *TACC3*-deficient/*p53*$^{+/+}$ fetal liver cells were unable to reconstitute hematopoiesis (0 survived/10 transplanted) under conditions in which *TACC3*-expressing cells were able to nearly completely rescue the irradiated mice (31/

33). However, fetal liver cells that were *TACC3* deficient and heterozygous or homozygous for *p53* deficiency were able to rescue hematopoiesis in approximately one-third to one-half of the recipient mice (7/23 and 2/4, respectively) (data not shown). The results are consistent with the concept that *p53* deficiency can completely correct the *TACC3* deficiency.

Lastly, we examined the ability to rescue the lymphoid lineages by transplanting fetal liver cells into sublethally irradiated *Jak3*-deficient mice. In these experiments, the

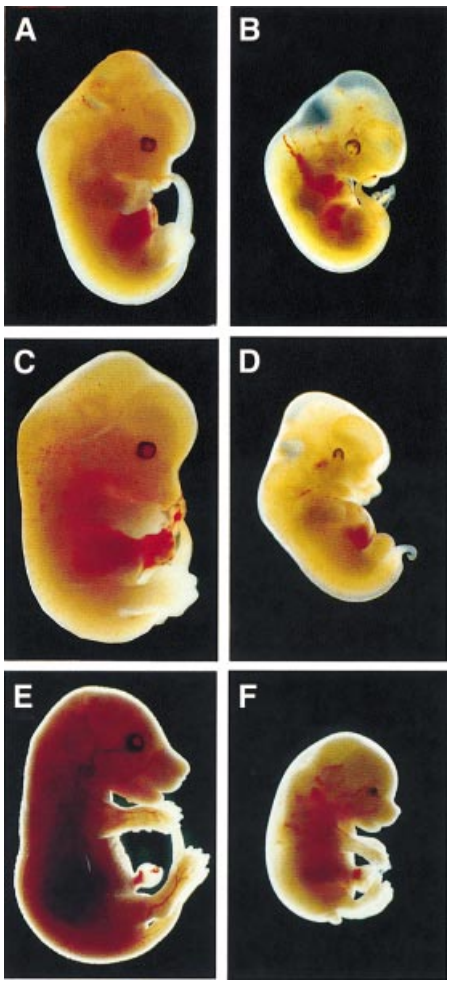

Fig. 4. Embryonic lethality and growth retardation due to *TACC3* deficiency. Embryos were dissected at days 12.5 (**A** and **B**), 13.5 (**C** and **D**) and 17 (**E** and **F**) p.c. from the embryo sacs and were photographed. The left panels show the morphology of wild-type embryos (A, C and E), while litter-mate mutant embryos on the right panels are characterized by a reduced size (B, D and F). The knockout embryo at E13.5 (D) displays a facial cleft.

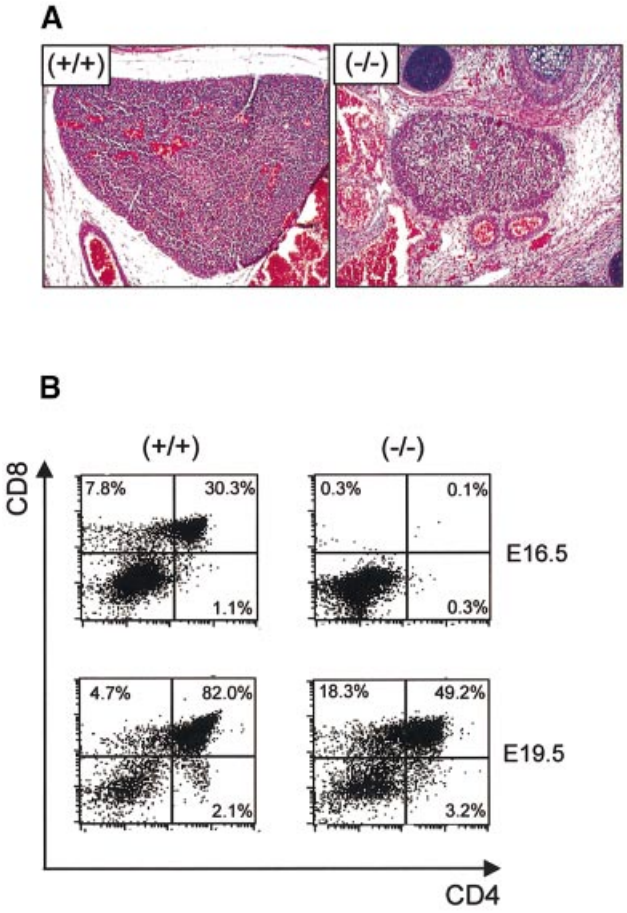

Fig. 5. Delayed generation of thymocytes in *TACC3*-deficient embryos. (**A**) Histological appearance of thymi from wild-type and *TACC3*-deficient embryos (E18.5). (**B**) Fetal thymocytes from wild-type and *TACC3*-deficient embryos were analyzed for the percentage of CD4/CD8 double positive and single positive cells at the stages of development indicated.

Table II. Colony-forming ability of hematopoietic progenitors from fetal livers of wild-type and TACC3-deficient embryos

Colony type	Cytokine(s)	Genotype			TACC3$^{(-/-)}$ versus TACC3$^{(+/+)}$ (%)
		TACC3$^{(+/+)}$	*TACC3*$^{(+/-)}$	TACC3$^{(-/-)}$	
CFU-Mix	SCF	88 ± 34.5 (n = 4)	94 ± 48 (n = 2)	1.4 ± 1.4 (n = 4)	1.6
CFU-Mix (BFU-E)	IL-3, IL-6, SCF, EPO	9 ± 5 (n = 5)	5 ± 3 (n = 6)	0.3 ± 0.3 (n = 6)	3.3
CFU-Mix (others)	IL-3, IL-6, SCF, EPO	39 ± 12 (n = 5)	36 ± 7 (n = 6)	2.2 ± 1.8 (n = 6)	5.6
BFU-E	IL-3, EPO	48 ± 21 (n = 5)	32 ± 13 (n = 6)	0.3 ± 0.3 (n = 6)	<1
CFU-E	EPO	888 ± 251 (n = 3)	900 ± 43 (n = 2)	168 ± 41 (n = 2)	18.9
CFU-Mix	IL-3	261 ± 99 (n = 3)	241 ± 113 (n = 4)	14 ± 8 (n = 4)	5.3
CFU-GM	GM-CSF	83 ± 29 (n = 3)	49 ± 9 (n = 4)	3 ± 3 (n = 4)	3.6
CFU-M	M-CSF	240 ± 90 (n = 3)	224 ± 78 (n = 2)	10.3 ± 9.5 (n = 2)	4.5
CFU-Meg	TPO	54 ± 6.7 (n = 2)	n.d.	0.0 ± 0.0 (n = 2)	0.0
CFU-Eo	IL-5	44 ± 17 (n = 3)	28 ± 2.8 (n = 2)	0.3 ± 0.3 (n = 2)	<1

Data represent the mean ± SD of numbers of colonies/10^5 fetal liver cells. n.d., not determined.

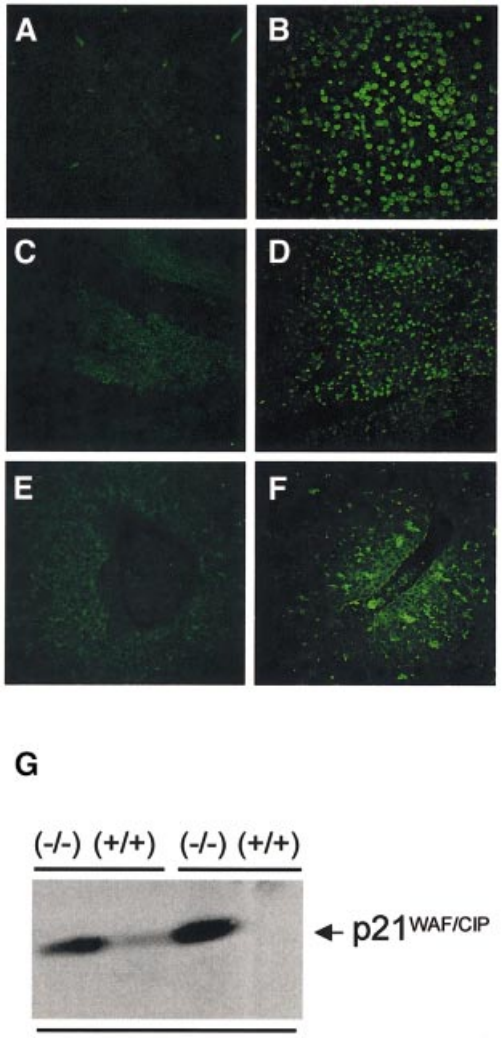

Fig. 6. Increased apoptosis and expression of $p21^{Waf1/Cip1}$ in fetal liver cells from *TACC3*-deficient embryos. Sagittal sections of E18.5 wild-type (**A**, **C** and **E**) and knockout embryos (**B**, **D** and **F**) were analyzed for the presence of apoptotic/TUNEL-positive (green) cells. Selected organs and structures shown include the forebrain cortex (A and B), gut (C and D) and fetal liver (E and F). (**G**) Protein levels of the cell cycle inhibitor $p21^{Waf1/Cip1}$ in fetal liver cell extracts from wild-type and knockout embryos (E17.5).

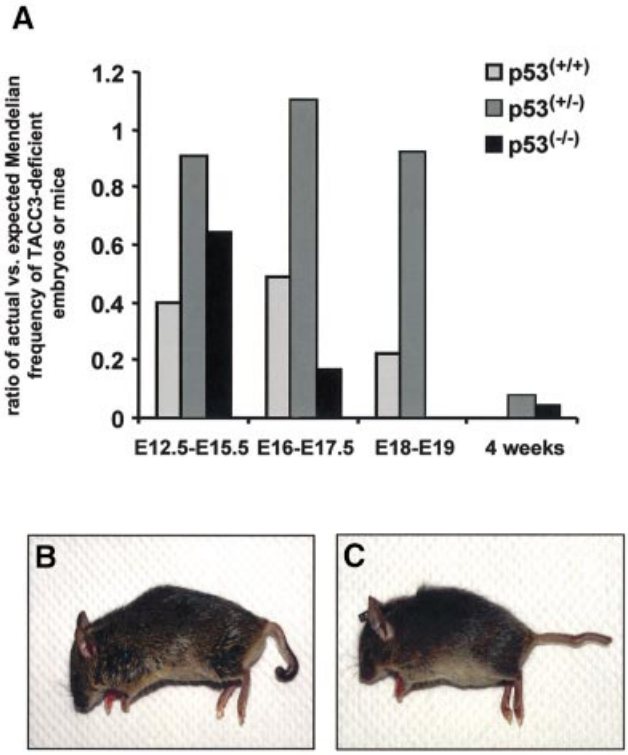

Fig. 7. Impact of p53 on the lethality of *TACC3*-deficient embryos. (**A**) The ratios of actual versus expected Mendelian frequencies were determined for *TACC3*-deficient embryos and mice dependent on the p53 background. Numbers of observed versus expected individuals alive: days 12.5–15.5 of embryonic development, 47/117 for $p53^{(+/+)}$, 10/11 for $p53^{(+/-)}$ and 7/11 for $p53^{(-/-)}$; days 16–17.5 of embryonic development, 23/47 for $p53^{(+/+)}$, 34/31 for $p53^{(+/-)}$ and 5/29 for $p53^{(-/-)}$; days 18–19 of embryonic development, 12/54 for $p53^{(+/+)}$, 12/13 for $p53^{(+/-)}$ and 0/12 for $p53^{(-/-)}$; mice, at least 4 weeks of age, 0/150 for $p53^{(+/+)}$, 8/107 for $p53^{(+/-)}$ and 3/67 for $p53^{(-/-)}$. *TACC3*-deficient mice that survive on a *p53* heterozygous (**B**) or *p53*-deficient (**C**) background are characterized by the occurrence of kinky or twisted tails.

number of peripheral B cells after 4 weeks is a sensitive marker for lymphoid reconstitution. *Jak3*-deficient mice have no detectable B cells in the peripheral blood (Nosaka *et al*., 1995) and reconstitution with wild-type fetal liver cells restores the peripheral B-cell count to values of $2.0–4.0 \times 10^6$/ml. As illustrated in Figure 8A, reconstitution of *Jak3*-deficient mice with fetal liver cells from embryos that contain one wild-type *TACC3* allele, independent of the *p53* phenotype, readily reconstituted the lymphoid system. In contrast, *TACC3*-deficient fetal livers were unable to reconstitute the lymphoid lineage. *TACC3* deficiency coupled with a heterozygous *p53* deficiency resulted in a low, but significant, level of reconstitution in each individual animal. More strikingly, *TACC3* deficiency coupled with a homozygous *p53* deficiency resulted in fetal liver cells with almost a wild-type capability of lymphoid reconstitution in individual recipients. The reconstituted B and T cells proliferated and expanded comparably with wild-type cells in response to either anti-CD40/IL-4 (Figure 8B) or anti-CD3/IL-2 (data not shown), respectively.

Lack of mitotic failure and normal centrosome numbers in TACC3-deficient hematopoietic cells

The *Drosophila TACC* homolog, *dTACC*, plays a critical role in mitotic spindle function during early embryogenesis (Gergely *et al*., 2000a). In particular, reduction of the amounts of dTACC protein causes mitotic defects giving rise to polyploidy/aneuploidy. To begin to investigate whether murine *TACC3* deficiency is associated with chromosomal abnormalities, karyotype analysis was performed on *TACC3*-deficient fetal liver cells. Among the ~20 *TACC3*-deficient mitotic fetal liver cells examined, all had normal karyotypes (data not shown). Culturing fetal liver cells from *TACC3*-deficient embryos for 4 months in IL-3/IL-6/SCF gave rise, in two independent cultures, to cell populations that grew more slowly than controls but which, like control cultures, contained c-kit/Sca1-positive cells with a normal cell cycle distribution. In these cultures, the cell populations contained an additional chromosome 12, with occasionally an additional Y chromosome,

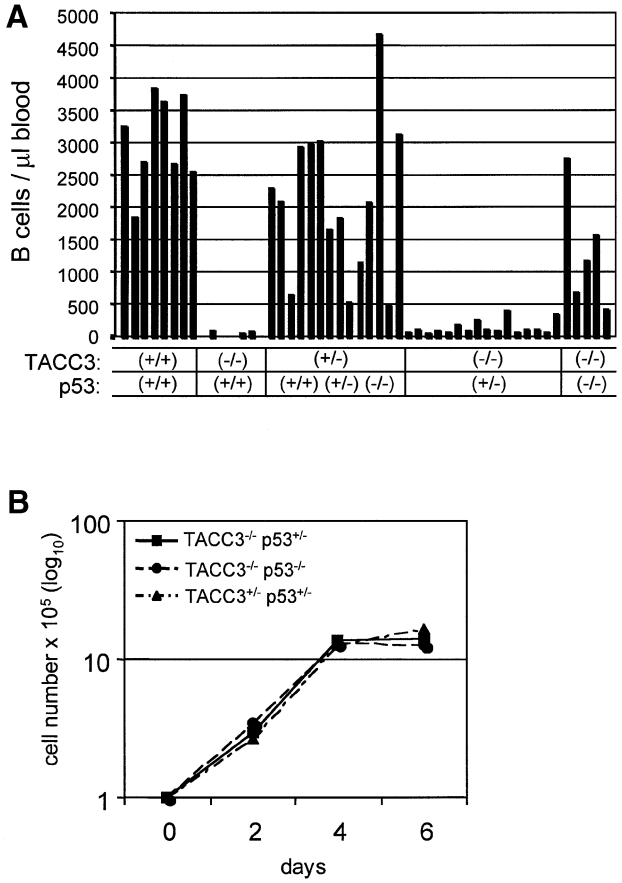

Fig. 8. *TACC3/p53*-deficient fetal liver cells rescue lymphoid cell development and expansion in *Jak3*-deficient mice. (**A**) Analysis of the number of B lymphocytes in the blood of individual *Jak3*-deficient mice transplanted with fetal liver cells from embryos with the indicated genotypes. (**B**) Growth kinetics of FACS-purified splenic B cells from transplanted *Jak3*-deficient mice in reponse to mitogenic treatment with αCD40 and IL-4. The number of viable cells was determined by Trypan Blue exclusion.

but without evidence of any gross chromosomal abnormalities. In comparison, cells from cultures of wild-type embryo fetal liver cells contained normal karyotypes.

To further assess karyotype stability, T-cell populations were expanded *in vitro* for 8 days in anti-CD3 and IL-2 from: (i) wild-type mice; (ii) *p53*-deficient mice; or (iii) *TACC3*-deficient mice with a homozygous or heterozygous *p53* deficiency. Following expansion, the cells were treated with colchicine for 6 h prior to preparing cytospin preparations for analysis. Cultures of T cells from individual wild-type mice showed a normal karyotype in four of the seven cultures. In the other three cases, 13/15 cells examined in each case had a normal karyotype. In one case the additional cells were hyperdiploid, in another the cells contained an X rearrangement or a loss of chromosome 18 with a gain of 13 or, in the last case, either a gain of Y or a gain of chromosome 8 and a loss of 18. Comparable ratios and types of chromosomal changes were observed in cultures of T cells from *p53*-deficient mice. In cultures of T cells from two *TACC3*-deficient, *p53*-deficient mice, one culture contained 5/17 cells with a normal karyotype while the second contained 9/15 cells with a normal karyotype. In one culture, four cells contained an additional chromosome 17, one cell contained an additional chromosome 6 and one cell was hyperdiploid. In the other culture, seven cells were hyperdiploid, four cells contained a gain of chromosome 17 with a loss of the Y chromosome and one cell contained a loss of the Y chromosome with a gain of chromosome 8. In cultures of T cells from four *TACC3*-deficient mice that were heterozygous for a deficiency of *p53*, the frequency of normal karotypes was 12/15, 9/15, 14/16 and 13/15. The abnormal karotypes were all single chromosome gains involving eight different chromosomes. We conclude from these observations that the absence of *TACC3* does not result in gross chromosomal alterations.

We also examined the possibility that *TACC3* deficiency might be associated with altered centrosome maintenance. However, the centrosome numbers, quantitated by γ-tubulin staining, of ~1100 *TACC3*-deficient fetal liver cells, enriched for progenitor cells by FACS sorting of c-kit-positive cells, were comparable to normal. Similarly, among the ~560 bone marrow-derived macrophages from *TACC3*-deficient/*p53* heterozygous mice examined, the centrosomal content was comparable to control cells.

Discussion

As demonstrated here, murine TACC3 protein is localized to the centrosome/spindle apparatus during the mitotic phase of the cell cycle and is cytoplasmic/perinuclear in interphase cells. These results are consistent with recent results with the human TACC3 protein (Gergely *et al.*, 2000b). In this regard TACC3 is similar to the other TACC family members, all of which have been shown to associate with the centrosome/spindle apparatus in mitotic cells, although differences exist in their precise localization on and around the spindle poles. Similarly, studies with the *Drosophila* protein (dTACC) (Gergely *et al.*, 2000a) have demonstrated that it is a centrosomal protein that is essential for spindle function in early embryos. Mechanistically, the localization of the TACC proteins to the centrosome/spindle apparatus is directed by the highly conserved coiled-coiled domain in the carboxyl region of the proteins (Gergely *et al.*, 2000a). The proteins with which the TACC domain interacts have yet to be defined although direct interaction with microtubules does not appear to occur (Gergely *et al.*, 2000a). However, recent studies in *Drosophila* show that dTACC interacts with the microtubulus-associated protein Msps/XMAP215 and targets it to the centrosome to regulate the stability of centrosomal microtubuli in meiotic cells and during early embryogenesis (Cullen and Ohkura, 2001; Lee *et al.*, 2001). A similar interaction exists between human TACC3 and ch-TOG, the evolutionarily conserved mammalian homolog of Msps, in mitotic cells (Lee *et al.*, 2001).

To further define the function of *TACC3* we created a strain of mice containing a null allele. The results demonstrate that *TACC3* has essential, non-redundant functions in specific cell lineages but is dispensable for other cell types including embryonic fibroblasts, which proliferate normally *in vivo* and *in vitro* without phenotypic alterations (data not shown). This specificity may be a consequence of the functional redundancy and expression of multiple family members by some cell types. For

example, in hematopoietic cells only TACC3 can be detected at high levels, whereas all TACC family members are expressed in fibroblasts, although at differing levels (data not shown). However, it should be noted that, although the TACC proteins have a highly conserved C-terminal coiled-coiled domain, there is no significant sequence homology throughout the remainder of the protein. To explore TACC functional redundancies it will be necessary to derive mutant strains of mice lacking the other family members.

The deficiency of *TACC3* results in a mid- to late embryonic lethality with evidence of abnormalities in several cell types, although our studies have focused primarily on the consequences of *TACC3* deficiency in hematopoietic cells. As illustrated, terminal differentiation of all the hematopoietic lineages can occur *in vivo* and *in vitro*, demonstrating that differentiation is not blocked and thereby ruling out a role for *TACC3* in differentiation. However, the ability of cells of all the hematopoietic lineages to proliferate is dramatically reduced, both *in vitro* in colony forming assays and *in vivo* in reconstitution experiments. The lack of amplification of progenitor cells could be due to restrictions to cell cycle progression and/or increased apoptosis. *In vivo* there are dramatically increased numbers of apoptotic cells, indicating that the primary basis for the lack of cells is an increased susceptibility to apoptosis. This is observed in both hematopoietic cells and cells in various tissues of *TACC3*-deficient embryos, including the neuroepithelium of the developing forebrain. In this regard, it should be noted that a significant fraction of *TACC3*-deficient embryos display exencephaly, a condition that is frequently associated with gene deficiencies that affect the frequency of apoptosis of neuroepithelial cells and, as a consequence, the process of neural tube closure (Copp *et al*., 2000).

Fetal liver cells of *TACC3*-deficient embryos expressed high levels of $p21^{Waf1/Cip1}$ protein. The transcription of the $p21^{Waf1/Cip1}$ gene is controlled in many situations by p53, suggesting that *TACC3* deficiency leads to increased p53 activity. The possibility that the increases in $p21^{Waf1/Cip1}$ are mediated by p53 is supported by the observation that $p21^{Waf1/Cip1}$ levels are present but decreased in *TACC3*-deficient, $p53^{(+/-)}$ embryos and absent in fetal liver cells from *TACC3*/*p53* null embryos (data not shown). The p53-induced expression of $p21^{Waf1/Cip1}$ is associated with the inhibition of cyclin–cdk complexes required for the transition from G_1 to S phase in fibroblasts, resulting in a G_1–S arrest (Brugarolas *et al*., 1995; Deng *et al*., 1995). More recently, p53 and $p21^{Waf1/Cip1}$ have been implicated in maintaining a G_2 checkpoint (Bunz *et al*., 1998). Analysis of sorted c-kit-positive progenitor cells from fetal liver has not revealed a G_1–S block, although a slight block in the S–G_2M transition may exist in comparing *TACC3*-deficient cells with wild-type cells (our unpublished data).

Studies with hematopoietic cells have also suggested the possibility that $p21^{Waf1/Cip1}$ may normally restrict entry of stem cells into the cell cycle and thereby preserve a stem cell population (Cheng *et al*., 2000). Thus, the high levels of $p21^{Waf1/Cip1}$ in *TACC3*-deficient fetal liver cells could be hypothesized to be suppressing stem cell proliferation. This possibility is being currently addressed by crossing the *TACC3* deficiency on a $p21^{Waf1/Cip1}$ null background. However, the high frequency of apoptotic cells would not be anticipated in this model. Consequently, we favor the possibility that the high levels of $p21^{Waf1/Cip1}$ reflect the functional activation of p53 and that it is the induction of apoptosis associated with p53 activation that is responsible for the inability to expand lineage progenitors. The role of $p21^{Waf1/Cip1}$ in apoptosis will also be assessed in the *TACC3*/$p21^{Waf1/Cip1}$ double deficient embryos. In this regard it is noteworthy that the apoptosis seen in *Brca1* exon 11-deficient embryos can be eliminated by *p53* deficiency, but not on a $p21^{Waf1/Cip1}$ null background (Xu *et al*., 2001).

An essential result in understanding *TACC3* function is the observation that the deficiency of *TACC3* in hematopoietic stem cells and myeloid and lymphoid stem cells can be compensated for by p53 deficiency. Specifically, *TACC3*/*p53*-deficient fetal liver stem cells, unlike *TACC3*-deficient cells, have the ability to proliferate and form colonies in response to cytokines (data not shown) and can reconstitute both the myeloid and lymphoid lineages in recipient mice. Moreover, myeloid and lymphoid lineage cells from the reconstituted mice function normally in a variety of cell responses. Rescue is also seen with a haploinsufficiency of p53, suggesting that simply lowering the levels of p53 is sufficient. Among the assays that we have used to measure stem cell function, the reconstitution of B cells in Jak3-deficient animals can provide the most quantitative information. As illustrated, *p53* heterozygously null fetal liver cells were less efficient than homozygously null cells, as measured by the number of B lymphocytes recovered following reconstitution of *Jak3*-deficient mice. Importantly, purified $TACC3^{(-/-)}$/$p53^{(+/-)}$ and $TACC3^{(-/-)}$/$p53^{(-/-)}$ B cells proliferated to the same extent as control B cells, indicating that stem cells and/or precursor cells represent the cell population that is mainly affected by *TACC3* deficiency *in vivo*. Since there is no compensatory upregulation of the other *TACC* family members (unpublished observation), the results indicate that *TACC3* is not essential for normal hematopoietic cell proliferation and consequently suggest the possibility that the sole function of *TACC3* in hematopoietic cells is to regulate p53 function.

The relatively few *TACC3*/*p53*-deficient mice that are obtained are phenotypically normal with the exception of male and female sterility (unpublished observation) and the presence of kinky or twisted tails. If *TACC3* were critical to the integrity of cell cycle progression, it might have been anticipated that these mice would be susceptible to karyotypic errors that would predispose the mice to cancer. For example, the embryonic lethality associated with DNA ligase IV (Frank *et al*., 2000) or *XRCC4* (Gao *et al*., 2000) deficiency can be rescued on a *p53*-deficient background but the double null mice rapidly succumb to B-cell lymphomas. Similarly, the embryonic lethality caused by a *Brca1* exon 11 deficiency, which is also associated with widespread apoptosis, can be rescued simply by elimination of one *p53* allele, giving rise to mice that mainly develop mammary tumors (Xu *et al*., 2001). In contrast, *TACC3*-deficient mice that are *p53* heterozygous or homozygous null do not have an apparent increase in tumors or decrease in their latency. Equally importantly, although the numbers are still small, *TACC3*/*p53* null mice develop tumors comparable to those seen with *p53*

deficiency alone. Higher numbers of rescued mice over longer periods of time will be necessary to determine whether subtle increases are present. With regard to chromosomal stability, initial studies have failed to identify gross chromosomal alterations when *TACC3*-deficient/*p53*-deficient or haploinsufficient T and B cells are expanded in tissue culture. One mechanism that can cause chromosomal aneuploidy and genetic instability relies on aberrant centrosome amplification (Brinkley, 2001), a situation, for example, typical of *BRCA1* exon 11 isoform-deficient cells (Xu *et al*., 2001). However, our initial studies have failed to detect abnormal centrosome numbers in enriched hematopoietic progenitor cells from *TACC3*-deficient embryos or in bone marrow-derived macrophages from $TACC3^{(-/-)}/p53^{(+/-)}$ mice.

In spite of the rescue of hematopoiesis, *p53* deficiency only marginally rescues the embryonic lethality associated with *TACC3* deficiency. This result indicates that *TACC3* has essential roles in other cell lineages and that these roles may be less related to regulating the function of p53 than in hematopoietic cells. In this regard it should be noted that the high frequency of exencephaly seen in *TACC3*-deficient embryos was not evident in the *TACC3*-deficient embryos on a $p53^{+/-}$ background (data not shown). As indicated, the absence of *TACC3* is associated with dramatically increased apoptosis in a number of cell lineages, including the neuroepithelium of the forebrain and the epithelial cells of the gut as well as other organs. Studies are ongoing to identify the cell types in which *p53* deficiency fails to eliminate apoptosis. In this regard, it is of note that *p53* deficiency can rescue the embryonic lethal phenotype of DNA ligase IV-deficient embryos and the associated neuronal apoptosis phenotype, but does not correct the lymphocyte developmental defects (Frank *et al*., 2000).

In contrast to the rescue obtained with *p53* deficiency, *ATM* deficiency is unable to rescue the embryonic lethality associated with *TACC3* deficiency (our unpublished observation). This is quite distinct from the lethality associated with DNA ligase IV deficiency, which is rescued by *ATM* deficiency (Lee *et al*., 2000; Sekiguchi *et al*., 2001). Importantly, similar to the results with *p53*, *ATM* deficiency rescued the embryonic lethality and neuronal apoptosis but not the lymphocyte development. One possible explanation for the differences could relate to the mechanisms by which p53 is functionally activated. DNA ligase IV or *XRCC4* deficiency would be anticipated to result in DNA damage that is detected through sensing mechanisms that require ATM for the functional activation of p53 and the subsequent induction of apoptosis. In contrast, *TACC3* deficiency may mediate the activation of p53 downstream of DNA damage and the pathways that transmit this recognition to p53, and may rather be associated with the sensing mechanisms involved in centrosome/spindle apparatus defects. At the molecular level, *TACC3* deficiency may activate an unknown pathway resulting in the functional activation of p53; alternatively, TACC3 protein may regulate p53 function directly or indirectly. In particular, it could be envisioned that TACC3 sequesters p53 during the mitotic phase of the cell cycle and thereby suppresses p53 function under conditions of normal cell cycle progression. In this model, the activation of p53 function during the mitotic phase of the cell cycle might require signals that disrupt the interaction. The possibility of a direct interaction is supported by recent studies that have shown that p53 localizes to the centrosomes and spindle apparatus in mitotic cells (Morris *et al*., 2000; Tarapore *et al*., 2001), and that inhibition of mitotic spindle function by nocodazole treatment leads to p53 displacement from centrosomes (Ciciarello *et al*., 2001). Studies are currently ongoing to determine whether and how TACC3 and p53 interact during the mitotic phase of the cell cycle. Initial biochemical results indicate that they do not associate directly; however, a co-localization between TACC3 and p53 at the spindle poles can be observed in mouse embryo fibroblasts in immunofluorescence studies (unpublished observation).

In summary, the results are consistent with a primary role for *TACC3* in hematopoietic cells in the regulation of p53 function. Since TACC3 protein is present only during the $S/G_2/M$ phases of the cell cycle in synchronized lymphocytes, it can be further hypothesized that TACC3 specifically regulates p53 activity during the mitotic phase of the cell cycle. It will be necessary to address the question of whether the amplification of TACC3 expression in transformed cells could provide another mechanism by which p53 function is compromised.

Materials and methods

Northern blot analysis

Northern blots with mRNAs from murine tissues were obtained from Clontech (Palo Alto, CA). Total RNA from IL-2-dependent cultured T lymphocytes (Moriggl *et al*., 1999) and hematopoietic tissues was separated on 1% formaldehyde–agarose gels. cDNA fragments of murine TACC3, TACC2 or GAPDH as a loading control, were labeled using [α-^{32}P]dCTP and a random priming labeling kit (Amersham, Arlington Heights, IL) and used as probes. Membranes were hybridized using a rapid hybridization solution (Amersham) followed by final stringent washes in 0.2 × SSC/0.1% SDS at 65°C.

Cell cycle analysis

For determination of cell cycle distribution, cells were stained with propidium iodide (50 μg/ml in 0.1% sodium citrate/0.1% Triton X-100) and treated with 2 μg/ml RNase for 30 min. The DNA content was assayed by flow cytometry (Becton Dickinson, Bedford, MA) and the percentage of cells within the S-phase of the cell cycle was quantified using ModFit software (Verify Software).

Antibodies, SDS–PAGE and western blotting

Antibodies against TACC3 were raised in rabbits using an N-terminal peptide (N18; amino acids 1–19) or a C-terminal peptide (C18; amino acids 603–620) of murine TACC3 as antigen. Total cell extracts were prepared in lysis buffer containing 0.5% NP-40 (Wang *et al*., 1996). For immunoprecipitation, protein extracts were incubated with N18 antiserum affinity purified by peptide chromatography. Immune complexes were analyzed by SDS–7.5% PAGE and transferred to nitrocellulose. Membranes were probed using the N18 or C18 antisera and visualized with the ECL detection system (Amersham). Expression of $p21^{Waf1/Cip1}$ was analyzed by direct western blotting using an antiserum (F5) (Santa Cruz Biotechnology Inc., Santa Cruz, CA).

Intracellular localization of TACC3

Exponentially growing mouse embryo fibroblasts were fixed with a 1:1 mixture of methanol and acetone for 20 min at –20°C. Cells were stained with rabbit anti-TACC3 antibodies (N18; 1:250; Upstate Biotechnology, Lake Placid, NY) and anti-rabbit-FITC (1:250) as secondary antibody (Santa Cruz Biotechnology). DNA was visualized using 4′,6-diamidino-2-phenylindole (DAPI; Sigma, St Louis, MO). Analysis was performed by confocal microscopy using a Leica DM-IRBE microscope together with Leica TCS-NT software.

Construction of TACC3 targeting vector and generation of TACC3-deficient mice

The *TACC3* gene was isolated from a 129 mouse/RW4 ES cell genomic BAC library (IncyteGenomics, Palo Alto, CA) using a 320 bp N-terminal *Bam*HI cDNA probe. A 9 kb *Eco*RI fragment identified by Southern blotting was subcloned into pBluescript II SK(+). For the *TACC3* targeting vector a 1.2 kb *Afl*II fragment containing parts of exon 3 and intron 3 was replaced with a neomycin resistance cassette described previously (van Deursen *et al*., 1991). A diphtheria toxin A (DTA) cassette mediating negative selection (Adachi *et al*., 1995) was inserted in the 3′-end of the *TACC3-neo* construct. Twenty micrograms of the *Sma*I linearized targeting vector were electroporated into E14 ES cells, which were grown under selection with 350 μg/ml geneticin (G418; Gibco, Rockville, MD). Clones were picked and expanded 7–9 days after electroporation. Correctly targeted ES clones were identified by Southern analysis (data not shown) and karyotypically normal clones were injected. Mice and embryos derived from two ES clones were analyzed in detail and identical phenotypes were observed. Conditions for blastocyst injection of ES cells and breeding to generate mice homozygous for the mutated *TACC3* gene were followed as described (van Deursen *et al*., 1993). Preliminary analysis indicates no differences in the phenotype of *TACC3* deficiency between the mixed 129/SvJ C57/Bl6 background and a pure C57/Bl6 background.

Genotyping of TACC3-deficient mice and embryos by PCR

Genomic DNA was amplified in 50 μl reactions using 2.5 U of Ampli*Taq* Gold (Perkin-Elmer, Branchburg, NJ) in PCR buffer with a final concentration of dNTPs at 0.2 mM and $MgCl_2$ at 2 mM. The PCR primer consisted of P1 primer (5′-CAGAGCCAGGCTAAGGCC-3′) at 0.4 μM, P2 primer (5′-CCTCACGCTTATTGGTCA-3′) at 0.2 μM and the neomycin primer P3 (5′-ATCTCCTGTCATCTCACCTTGCT-3′) at 0.4 μM. The PCR cycle profile was as follows: one cycle at 94°C for 10 min followed by 35 cycles at 94°C for 1 min, 55°C for 1 min, 72°C for 1 min with 5 s auto-extension in every cycle; and finally one cycle at 72°C for 10 min. A 240 bp fragment indicates the presence of the wild-type allele, whereas an 800 bp fragment is amplified from the mutated allele.

Generation of TACC3/p53-deficient mice

$TACC3^{(+/-)}$ and $p53^{(-/-)}$ mice (Jacks *et al*., 1994) were bred to generate $TACC3^{(+/-)}p53^{(+/-)}$ mice on a mixed background (129/Ola-C57BL/6), which were intercrossed to finally generate $TACC3^{(-/-)}p53^{(+/-)}$ or $TACC3^{(-/-)}p53^{(-/-)}$ mice. Genotypes for *TACC3* and *p53* were determined by genomic PCR.

Histology and TUNEL staining

Embryos were fixed in 10% phosphate-buffered formalin (Fisher, Hernando, MS), paraffin embedded and 5 μm sections were prepared. Sections were stained using hematoxylin and eosin. Cells undergoing apoptosis were identified by TUNEL staining using an apoptosis detection kit (Roche, Indianapolis, IN).

Fetal liver colony assays

Fetal liver cells were prepared from livers of E13–E18.5 embryos in α-MEM medium (Gibco, Rockville, MD) containing 2% fetal bovine serum (Hyclone, Logan, UT). Diluted cell suspensions and recombinant cytokines specific for the assays described below were mixed with Methocult 3230 (StemCell Technologies, Vancouver, Canada) giving a final concentration of 0.9% methylcellulose. Assays were plated in 35 mm culture dishes in duplicate and cultured at 37°C. For the BFU-E (erythroid lineage burst-forming units) assay, 2×10^5 cells/dish were cultured in 3 U/ml recombinant human erythropoietin (rhEPO) and 10 ng/ml recombinant murine IL-3 (rmIL-3) and colonies consisting of more primitive erythroid progenitors were scored at day 8. For the CFU-E (erythroid colony-forming units) assay, 2×10^5 cells/dish were cultured in 0.2 U/ml rhEPO, and colonies consisting of more mature erythroblasts were scored at day 3. For the CFU-Mix assay (multi-lineage colonies), 1.5×10^4 cells/dish were cultured in a combination of 3 U/ml rhEPO, 10 ng/ml rmIL-3, 10 ng/ml rhIL-6 and 10 ng/ml recombinant murine stem cell factor (rmSCF), and different kinds of colony types were scored between days 8 and 12. Alternatively, rmIL-3 or rmSCF alone was used for the CFU-Mix assay, allowing the generation of colonies dependent on IL-3 or SCF. For the CFU-GM assay (myeloid-lineage colonies) and CFU-M assay (monocytic-lineage colonies) 1.5×10^4–5×10^4 cells/dish were cultured in 10 ng/ml recombinant murine granulocyte/macrophage colony-stimulating factor (rmGM-CSF) or 10 ng/ml recombinant murine colony-stimulating factor-1 (rmCSF-1), respectively, and colonies were scored between days 8 and 12. For the CFU-Meg assay (megakaryocytic colonies), 5×10^5 cells/dish were cultured in 50 ng/ml rhTPO (recombinant human thrombopoietin) and colonies were scored at day 8. For the CFU-Eo assay (colonies containing eosinophils), 2×10^5 cells/dish were cultured in 20 ng/ml rmIL-5, and colonies were scored at day 18. Recombinant human EPO and TPO were from Amgen (Thousand Oaks, CA) and Genzyme (Cambridge, MA), respectively, whereas all other cytokines were obtained from R&D Systems (Minneapolis, MN).

Flow cytometry

Fetal thymi were obtained from embryos at days 16.5–19.5 p.c. Single cell suspensions were prepared in PBS supplemented with 2% bovine serum albumin. Non-specific staining was minimized by blocking Fc receptor binding with rat anti-mouse CD16/CD32 antibodies (Pharmingen, San Diego, CA). Cells were then stained with phycoerythrin (PE)-conjugated anti-CD8 and cychrome (Cy)-conjugated anti-CD4 (Pharmingen, San Diego, CA) or appropriate isotype control antibodies. Subsequently, cells were washed and cell surface expression of the markers was analyzed in a Becton-Dickinson FACScan in two-color mode using CellQuest software.

Reconstitution of hematopoietic lineages and mitogenic stimulation of purified B cells

Fetal liver cells of different genotypes were isolated and used to reconstitute lethally irradiated (1100 Rad) wild-type mice or sublethally irradiated (450 Rad) JAK3-deficient mice, which display a severe combined immunodeficiency (SCID)-like phenotype due to the absence of functional lymphocytes (Nosaka *et al*., 1995). In particular, since JAK3-deficient mice lack peripheral B cells they represent an excellent model system for hematopoietic transplantation studies leading to the reconstitution of the B-cell compartment. Fetal liver cells were injected into the tail blood vein of recipient mice in 550 μl of PBS containing 2% fetal bovine serum. After 4 weeks the absolute numbers of B lymphocytes in the blood of reconstituted JAK3-deficient animals were determined as described previously (Bunting *et al*., 1998). Splenic B cells from reconstituted mice were purified by FACS ($B220^+$/$Thy1.2^-$; 98% purity) and expanded *in vitro* after stimulation with αCD40 (0.5 μg/ml; Pharmingen) and 100 ng/ml IL-4 (R&D Systems).

Acknowledgements

The expert technical assistance of Kristen Rothammer is gratefully acknowledged. The authors would like to thank Christie Nagy and John Raucci for their expert assistance in generating TACC3-deficient mice and the personnel of the Animal Resources Center for care and monitoring of animals. The support of Neena Carpino, Mahnaz Paktinat, Richard Cross, Sam Lucas, Susan Ragsdale and Ken Barnes in FACS, cell cycle and karyotypic analysis and confocal microscopy, respectively, is gratefully appreciated. Special thanks to Jordan Raff for sharing unpublished observations and to laboratory members and colleagues, in particular Richard Moriggl, Gerry Zambetti, Paul Ney and John Cleveland, for experimental advice, suggestions and fruitful discussions. Mice deficient for p53 or ATM were kindly provided by Tyler Jacks/Gerry Zambetti and Peter McKinnon, respectively. This work is supported by the Cancer Center CORE grant CA21765, by the grant RO1 DK42932 to J.N.I., by grant PO1 HL53749 and by the American Lebanese Syrian Associated Charities (ALSAC).

References

Adachi,M., Suematsu,S., Kondo,T., Ogasawara,J., Tanaka,T., Yoshida,N. and Nagata,S. (1995) Targeted mutation in the Fas gene causes hyperplasia in peripheral lymphoid organs and liver. *Nature Genet.*, **11**, 294–300.

Brinkley,B.R. (2001) Managing the centrosome numbers game: from chaos to stability in cancer cell division. *Trends Cell Biol.*, **11**, 18–21.

Brugarolas,J., Chandrasekaran,C., Gordon,J.I., Beach,D., Jacks,T. and Hannon,G.J. (1995) Radiation-induced cell cycle arrest compromised by p21 deficiency. *Nature* **377**, 552–557.

Bunting,K.D., Sangster,M.Y., Ihle,J.N. and Sorrentino,B.P. (1998) Restoration of lymphocyte function in Janus kinase 3-deficient mice by retroviral-mediated gene transfer. *Nature Med.*, **4**, 58–64.

Bunz,F., Dutriaux,A., Lengauer,C., Waldman,T., Zhou,S., Brown,J.P., Sedivy,J.M., Kinzler,K.W. and Vogelstein,B. (1998) Requirement for

p53 and p21 to sustain G_2 arrest after DNA damage. *Science*, **282**, 1497–1501.

Chen,H.M., Schmeichel,K.L., Mian,I.S., Lelievre,S., Petersen,O.W. and Bissell,M.J. (2000) AZU-1: a candidate breast tumor suppressor and biomarker for tumor progression. *Mol. Biol. Cell*, **11**, 1357–1367.

Cheng,T., Rodrigues,N., Shen,H., Yang,Y., Dombkowski,D., Sykes,M. and Scadden,D.T. (2000) Hematopoietic stem cell quiescence maintained by $p21^{cip1/waf1}$. *Science*, **287**, 1804–1808.

Ciciarello,M., Mangiacasale,R., Casenghi,M., Zaira,L.M., D'Angelo,M., Soddu,S., Lavia,P. and Cundari,E. (2001) p53 displacement from centrosomes and p53-mediated G_1 arrest following transient inhibition of the mitotic spindle. *J. Biol. Chem.*, **276**, 19205–19213.

Compton,D.A. (2000) Spindle assembly in animal cells. *Annu. Rev. Biochem.*, **69**, 95–114.

Copp,A., Cogram,P., Fleming,A., Gerrelli,D., Henderson,D., Hynes,A., Kolatsi-Joannou,M., Murdoch,J. and Ybot-Gonzalez,P. (2000) Neurulation and neural tube closure defects. *Methods Mol. Biol.*, **136**, 135–160.

Cullen,C.F. and Ohkura,H. (2001) Msps protein is localized to acentrosomal poles to ensure bipolarity of *Drosophila* meiotic spindles. *Nature Cell Biol.*, **3**, 637–642.

Deng,C., Zhang,P., Harper,J.W., Elledge,S.J. and Leder,P. (1995) Mice lacking $p21^{CIP1/WAF1}$ undergo normal development, but are defective in G_1 checkpoint control. *Cell*, **82**, 675–684.

Frank,K.M. *et al* (2000) DNA ligase IV deficiency in mice leads to defective neurogenesis and embryonic lethality via the p53 pathway. *Mol. Cell*, **5**, 993–1002.

Gao,Y. *et al* (2000) Interplay of p53 and DNA-repair protein XRCC4 in tumorigenesis, genomic stability and development. *Nature*, **404**, 897–900.

Gergely,F., Kidd,D., Jeffers,K., Wakefield,J.G. and Raff,J.W. (2000a) D-TACC: a novel centrosomal protein required for normal spindle function in the early *Drosophila* embryo. *EMBO J.*, **19**, 241–252.

Gergely,F., Karlsson,C., Still,I., Cowell,J., Kilmartin,J. and Raff,J.W. (2000b) The TACC domain identifies a family of centrosomal proteins that can interact with microtubules. *Proc. Natl Acad. Sci. USA*, **97**, 14352–14357.

Groisman,I., Huang,Y.S., Mendez,R., Cao,Q., Theurkauf,W. and Richter,J.D. (2000) CPEB, maskin, and cyclin B1 mRNA at the mitotic apparatus: implications for local translational control of cell division. *Cell*, **103**, 435–447.

Hsu,L.C. and White,R.L. (1998) BRCA1 is associated with the centrosome during mitosis. *Proc. Natl Acad. Sci. USA*, **95**, 12983–12988.

Jacks,T., Remington,L., Williams,B.O., Schmitt,E.M., Halachmi,S., Bronson,R.T. and Weinberg,R.A. (1994) Tumor spectrum analysis in p53-mutant mice. *Curr. Biol.*, **4**, 1–7.

Lee,M.J., Gergely,F., Jeffers,K., Peak-Chew,S.Y. and Raff,J.W. (2001) Msps/XMAP215 interacts with the centrosomal protein D-TACC to regulate microtubule behaviour. *Nature Cell Biol.*, **3**, 643–649.

Lee,Y., Barnes,D.E., Lindahl,T. and McKinnon,P.J. (2000) Defective neurogenesis resulting from DNA ligase IV deficiency requires Atm. *Genes Dev.*, **14**, 2576–2580.

McKeveney,P.J., Hodges,V.M., Mullan,R.N., Maxwell,P., Simpson,D., Thompson,A., Winter,P.C., Lappin,T.R. and Maxwell,A.P. (2001) Characterization and localization of expression of an erythropoietin-induced gene, ERIC-1/TACC3, identified in erythroid precursor cells. *Br. J. Haematol.*, **112**, 1016–1024.

Moriggl,R. *et al.* (1999) Stat5 is required for IL-2 induced cell cycle progression of peripheral T cells. *Immunity*, **10**, 249–259.

Moritz,M. and Agard,D.A. (2001) γ-tubulin complexes and microtubule nucleation. *Curr. Opin. Struct. Biol.*, **11**, 174–181.

Morris,V.B., Brammall,J., Noble,J. and Reddel,R. (2000) p53 localizes to the centrosomes and spindles of mitotic cells in the embryonic chick epiblast, human cell lines, and a human primary culture: An immunofluorescence study. *Exp. Cell Res.*, **256**, 122–130.

Nosaka,T., van Deursen,J.M.A., Tripp,R.A., Thierfelder,W.E., Witthuhn, B.A., McMickle,A.P., Doherty,P.C., Grosveld,G.C. and Ihle,J.N. (1995) Defective lymphoid development in mice lacking Jak3. *Science*, **270**, 800–802.

Pu,J.J., Li,C., Rodriguez,M. and Banerjee,D. (2001) Cloning and structural characterization of ECTACC, a new member of the transforming acidic coiled coil (TACC) gene family: cDNA sequence and expression analysis in human microvascular endothelial cells. *Cytokine*, **13**, 129–137.

Sadek,C.M., Jalaguier,S., Feeney,E.P., Aitola,M., Damdimopoulos,A.E., Pelto-Huikko,M. and Gustafsson,J. (2000) Isolation and characterization of AINT: a novel ARNT interacting protein expressed during murine embryonic development. *Mech. Dev.*, **97**, 13–26.

Sekiguchi,J. *et al.* (2001) Genetic interactions between ATM and the nonhomologous end-joining factors in genomic stability and development. *Proc. Natl Acad. Sci. USA*, **98**, 3243–3248.

Shah,J.V. and Cleveland,D.W. (2000) Waiting for anaphase: Mad2 and the spindle assembly checkpoint. *Cell*, **103**, 997–1000.

Stebbins-Boaz,B., Cao,Q., de Moor,C.H., Mendez,R. and Richter,J.D. (1999) Maskin is a CPEB-associated factor that transiently interacts with elF-4E. *Mol. Cell*, **4**, 1017–1027.

Still,I.H., Hamilton,M., Vince,P., Wolfman,A. and Cowell,J.K. (1999a) Cloning of TACC1, an embryonically expressed, potentially transforming coiled coil containing gene, from the 8p11 breast cancer amplicon. *Oncogene*, **18**, 4032–4038.

Still,I.H., Vince,P. and Cowell,J.K. (1999b) The third member of the transforming acidic coiled coil-containing gene family, TACC3, maps in 4p16, close to translocation breakpoints in multiple myeloma, and is upregulated in various cancer cell lines. *Genomics*, **58**, 165–170.

Tarapore,P., Tokuyama,Y., Horn,H.F. and Fukasawa,K. (2001) Difference in the centrosome duplication regulatory activity among p53 'hot spot' mutants: potential role of Ser315 phosphorylation-dependent centrosome binding of p53. *Oncogene*, **20**, 6851–6863.

Thomas,R.C., Edwards,M.J. and Marks,R. (1996) Translocation of the retinoblastoma gene product during mitosis. *Exp. Cell Res.*, **223**, 227–232.

van Deursen,J., Lovell-Badge,R., Oerlemans,F., Schepens,J. and Wieringa,B. (1991) Modulation of gene activity by consecutive gene targeting of one creatine kinase M allele in mouse embryonic stem cells. *Nucleic Acids Res.*, **19**, 2637–2643.

van Deursen,J., Heerschap,A., Oerlemans,F., Ruitenbeek,W., Jap,P., ter Laak,H. and Wieringa,B. (1993) Skeletal muscles of mice deficient in muscle creatine kinase lack burst activity. *Cell*, **74**, 621–631.

Wang,D., Stravopodis,D., Teglund,S., Kitazawa,J. and Ihle,J.N. (1996) Naturally occurring dominant negative variants of Stat5. *Mol. Cell. Biol.*, **16**, 6141–6148.

Xu,X., Qiao,W., Linke,S.P., Cao,L., Li,W.M., Furth,P.A., Harris,C.C. and Deng,C.X. (2001) Genetic interactions between tumor suppressors Brca1 and p53 in apoptosis, cell cycle and tumorigenesis. *Nature Genet.*, **28**, 266–271.

Received September 26, 2001; revised December 19, 2001; accepted December 20, 2001